Phase Behavior of Hydrogen-Bonded Polymer−Surfactant Mixtures in Selective Solvent

Isamu Akiba,* Hiroyasu Masunaga, Kanako Sasaki, Yeonhwan Jeong, and Kazuo Sakurai

Faculty of Environmental Engineering, The University of Kitakyushu, 1-1 Hibikino, Wakamatsu, Kitakyushu, Fukuoka 808-0135, Japan

Received August 17, 2004; Revised Manuscript Received October 20, 2004

ABSTRACT: The phase behavior of the hydrogen-bonded poly(*N*-vinylpyrrolidone)−*p*-dodecylphenol (PVP−PDP) mixture in toluene solution was investigated. When the concentration of the PVP−PDP mixture in the toluene solution is lower than 10 wt %, the solution formed a clear sol. In the sol situation, a micelle consisting of the PVP core and the PDP shell was formed. Comparison of small-angle X-ray scattering (SAXS) measurements with theoretical scattering profiles calculated for some models indicated that the PVP−PDP micelle took a rodlike form with a 12 nm cross-sectional radius in the sol situation. On the other hand, the toluene solution of the PVP−PDP mixture formed a gel when the concentration of PVP−PDP in the solution is 10 wt % or above. SAXS analysis indicated that the rodlike structure of the PVP−PDP aggregate was maintained in the gel situation.

1. Introduction

Polymer−surfactant mixtures or complexes have attracted attention due to their interesting properties and potential applications.[1−8] The formations of polymer−surfactant aggregates are driven by attractive interactions, such as electrostatic interaction and hydrogen bond, between polymer chains and the polar headgroups of the surfactants. Because of such associations between a polymer and a surfactant, the polymer−surfactant mixtures form comblike complexes which have a *main chain* of the polymer and short *side chains* of hydrophobic groups of the surfactants.[1−8] Since the *side chains* are noncovalently connected with the *main chain* in the comblike complex, the properties or phase behavior in the comblike polymer−surfactant complexes should be much different from those of the covalently bonded comblike polymers.

It has been well-known that environmental changes or external stimuli cause drastic changes in conformation and molecular assembly of the comblike polymer−surfactant aggregates due to the noncovalent bond and large difference of polarity between polymer and surfactant.[3a,7b,8−10] When the polymer−surfactant systems are dissolved in a selective solvent for the *side chains* of the comblike complexes, the stiffening of the *main chains* of the comblike complexes is induced because of spatial constraint and strong associations between the polymer and surfactant.[11] The solvent-induced stiffening of the *main chain* of the polymer−surfactant complexes would provide anisotropy to the shape of the aggregates of the complexes in the selective solvent. The lyotropic phase behavior of the polymer−surfactant system induced by the selective solvent is of great interest.

The aim of the present study is to investigate on aggregation behavior of the polymer−surfactant mixtures in selective solvent for the *side chains* of the comblike complex. For this purpose, we chose here toluene solution of the polymer−surfactant mixture consisting of poly(*N*-vinylpyrrolidone) (PVP) and *p*-dodecylphenol (PDP) because the repeating unit of the PVP forms an extremely strong hydrogen bond with hydroxy groups of phenols.[12]

2. Experimental Section

PVP (M_w = 3.6 × 10^5 g mol^{-1}) and PDP were purchased from Tokyo Chemical Industry Co., Ltd., and Kanto Chemical Co., Ltd., respectively. They were used as obtained. They were weighted to repeating unit of PVP:PDP = 1:1 (mol:mol) and dissolved in methanol at 10 wt %. The reason why we chose this molar ratio is because the polymer−surfactant mixtures generally take comblike aggregates at 1:1 stoichiometry between repeating unit of polymer and surfactant. After complete dissolution of the solutes, the solvent was evaporated. The resulting samples were further dried in reduced pressure for 1 day. The PVP−PDP mixture was transparent. The PVP−PDP mixture was dissolved in toluene at desired concentrations. Clear solutions were obtained irrespective of the concentrations. The solutions were represented as PVP−PDP(x), where x denotes the concentration (wt %) of the PVP−PDP mixture.

The gel-to-sol transition temperatures of the PVP−PDP(x) were determined by visible inspection. The PVP−PDP(x)s were packed in test tubes. The tubes were placed at desired temperature for 5 min. After that, the situations of the solutions were determined by "test tube tilting" method.[13]

Fourier transform infrared (FTIR) spectra of PVP, PDP, and PVP−PDP(x) were measured using a Perkin-Elmer GX-2000R FTIR spectrometer at a resolution of 2 cm^{-1}. PVP film or the other liquid samples were sandwiched with KBr plates and compression-molded to KBr disks for FTIR measurements.

Dynamic light scattering (DLS) measurements were performed using an Otsuka Electric Co., Ltd., DLS-7000 at room temperature. A He−Ne laser (632.5 nm) was used as a light source.

Small-angle X-ray scattering (SAXS) experiments were carried out at the BL45XU station at SPring-8, Japan. Two-dimensional SAXS patterns were obtained by cold CCD. One-dimensional SAXS profiles ($I(q)$ vs q) were converted from the two-dimensional patterns by circular averaging. Here, $I(q)$ is the scattering intensity and q is the magnitude of scattering vector defined as eq 1:

$$q = (4\pi/\lambda)\sin(\theta/2) \quad (1)$$

* Corresponding author: phone +81-93-695-3295; Fax +81-93-695-3385; e-mail akiba@env.kitakyu-u.ac.jp.

10.1021/ma0483118 CCC: $27.50
Published on Web 12/02/2004

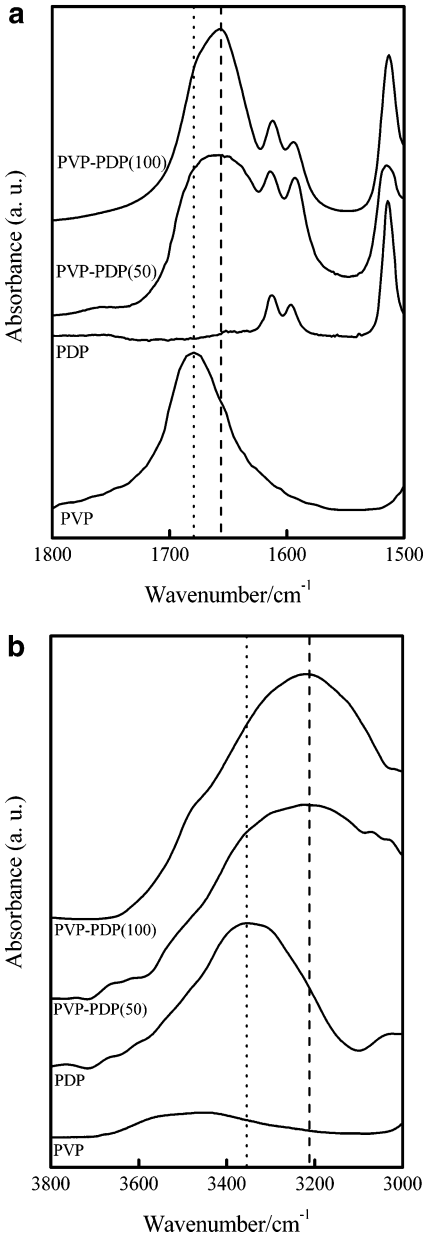

Figure 1. FTIR spectra for PVP, PDP, and 1:1 stoichiometric mixture of PVP−PDP: (a) carbonyl stretching region and (b) hydroxy stretching region.

where λ is the wavelength of the X-ray and θ is the scattering angle.

3. Results and Discussion

Figure 1 shows FTIR spectra of PVP, PDP, PVP−PDP(50), and PVP−PDP(100). It has been well-known that the nonassociating and hydrogen-bonding carbonyl groups of PVP show absorbance peaks at 1670 and 1650 cm^{-1}, respectively.[12] As can be seen in Figure 1a, absorbance peak of carbonyl group of PVP is shifted from 1670 to 1650 cm^{-1} in the PVP−PDP(100) and PVP−PDP(50). Because the PDP does not show any absorbance peaks in this region, the shift of the absorbance peak strongly suggests the formation of hydrogen bond between carbonyl group of PVP and hydroxy group of PDP in bulk and the toluene solution. In addition, the PVP−PDP(100) and PVP−PDP(50) show an absorbance peak at 3250 cm^{-1} in the hydroxy stretching band, although the PDP shows absorbance peak at 3500 cm^{-1} as shown in Figure 1b. The absorbance peaks at 3250 and 3500 cm^{-1} are attributed to the hydrogen-bonded and free hydroxy group, respectively. Summarizing the results of changes in the FTIR spectra, a hydrogen bond is formed between the carbonyl group of the PVP and the hydroxy group of the PDP in bulk and the toluene solution. The hydrogen bond between the PVP and PDP in the toluene solution should strongly affect the phase behavior of the solution of the PVP−PDP mixture.

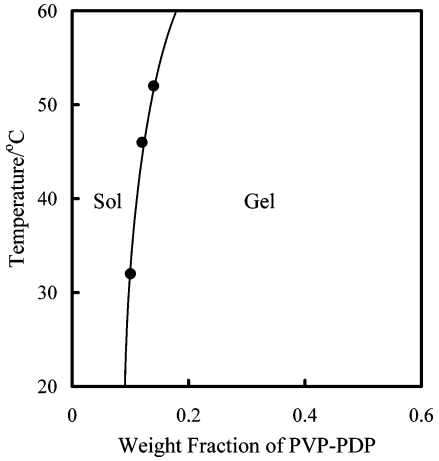

Figure 2. Appearance of toluene solution of the PVP−PDP mixture.

Figure 2 shows the appearance of the toluene solution of the PVP−PDP mixture. Although the PVP alone is insoluble in toluene, the PVP−PDP mixture forms the homogeneous toluene solution due to the hydrogen-bonded aggregation with toluene-soluble PDP. The PVP−PDP($x<10$) solutions take sol situations, although the PVP−PDP($x\geq10$) solutions form gels at room temperature. The gels of the PVP−PDP($x\geq10$) shows a gel-to-sol transition with elevating temperature. From the DLS measurements, the hydrodynamic radius (R_h) of the solute in the sol situation of the solution of the PVP−PDP mixture is estimated to 39 nm. The R_h of the PDP is not estimated because the PDP is too small to give rise to enough scattering intensity. On the other hand, the R_h of the PVP in aqueous solution is estimated to be 16 nm. Because the PVP is insoluble in toluene, the R_h of the PVP is measured for the aqueous solution in which the PVP should be sufficiently solvated. Therefore, the actual R_h of the PVP in toluene solution should be smaller than 16 nm. Since the R_h of the solute in the toluene solution of the PVP−PDP mixture is much greater than those of PVP and PDP, the PVP and PDP form a molecular aggregate in the toluene solution. Since the PVP is insoluble in toluene, the PVP−PDP aggregate in the solution should form micelle consisting of PVP core and shell of hydrocarbon chains of PDP. In addition, the PVP−PDP($x\geq10$) form gels as shown in Figure 2. Therefore, it is considered that the micelle of the PVP−PDP aggregate should take anisotropic form, such as rodlike structure.

Figure 3 shows SAXS profiles for the PVP−PDP(x = 5.0, 10, 20, 50, and 100) at room temperature. The PVP−PDP(100) and PVP−PDP(50) show scattering peaks at q = 2.25 and 0.68 nm^{-1}, respectively. In general, hydrogen-bonded polymer−surfactant mixtures in bulk form a mesomorphically ordered phase like a comblike polymer. Therefore, these peaks of the PVP−PDP(100) and PVP−PDP(50) are caused from the ordered phase of the comblike PVP−PDP aggregates. On the other hand, when the concentration of the

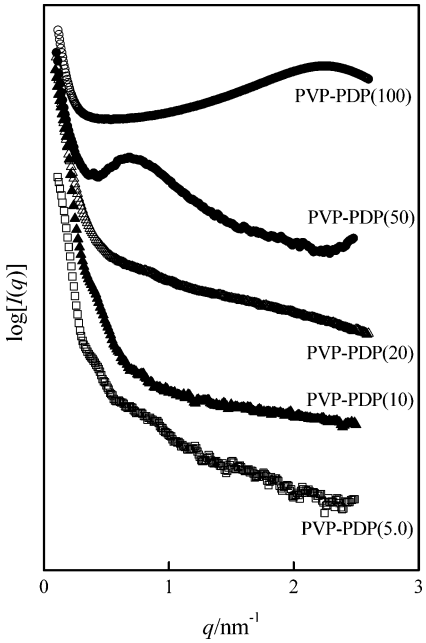

Figure 3. SAXS profiles of toluene solutions of PVP−PDP mixture with various concentration.

solution of the PVP−PDP mixture is lower than 50 wt %, the scattering peak is no longer detectable. Therefore, the ordered phase structure of comblike complex is not maintained in the solution of the PVP−PDP mixture when the concentration is lower than 50 wt %. However, strong X-ray scatterings in the small-angle regions still remain in the solution of the PVP−PDP mixture. Especially, the PVP−PDP(5.0) (sol) and PVP−PDP(10) (gel in the vicinity of gelation concentration) obviously show the SAXS profiles similar to that from isolated particle, such as micelle. Hence, the PVP and PDP should form the molecular aggregate in the toluene solution. This result corresponds to the DLS result as mentioned above. Then, we investigate the aggregation behavior of the PVP−PDP mixture in the toluene solution by analyzing the SAXS profiles of the PVP−PDP(5.0) and PVP−PDP(10).

The SAXS profiles of the micelle solutions are related to the shapes of the micelles. In the case that the contribution of interaction between the micelles is negligible, the SAXS intensity $I(q)$ from an isolated micelle is given by eq 2[14−18]

$$I(q) = fnP(q) \tag{2}$$

where n is the number density of micelle, $P(q)$ is the form factor of micelle, and f is the correction factor. The f is needed because the SAXS intensity of the experimental data is obtained in arbitrary unit. For isolated spherical micelle, $P(q)$ is given by eq 3[14−18]

$$P(q) = \Delta\rho^2V^2[3\{\sin(qR) - qR\cos(qR)\}/(qR)^3] \tag{3}$$

where $\Delta\rho$ is difference of electron density between the micelle and solvent and R is radius of the spherical micelle. The R is related to radius of gyration (R_g) of micelle by eq 4: [14]

$$R_g^2 = (3/5)R^2 \tag{4}$$

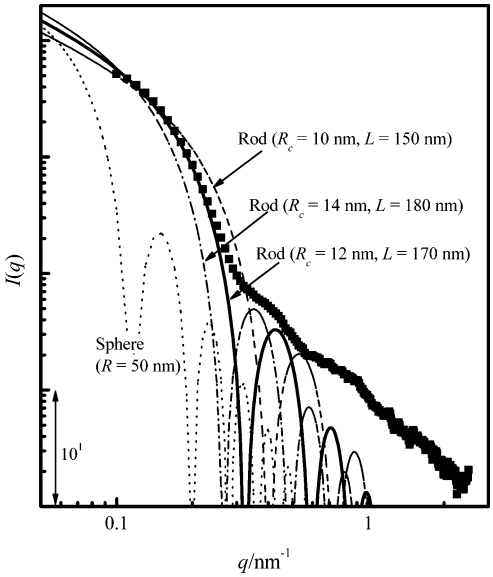

Figure 4. Experimental and calculated SAXS profiles for PVP−PDP(5.0). Dashed line is calculated by assuming spherical micelle with R = 50 nm, and solid line is calculated by assuming rodlike micelle with R_c = 12 nm and L = 170 nm.

On the other hand, for the rodlike micelle, $P(q)$ is expressed by eq 5[14−18]

$$P(q) = \{4\pi/(qL)\}\Delta\rho^2V^2[J_1(qR_c)/(qR_c)]^2 \tag{5}$$

where L is rod length, R_c is the radius of cross section of the rod, and J_1 is the Bessel function of the first order. The R_c and L are related to the R_g by eq 6:[14]

$$R_g^2 = R_c^2/2 + L^2/12 \tag{6}$$

The R_g is related to R_h by $R_g/R_h = 0.775$ for a sphere form and 1.25 for a relatively short rod.[19] Therefore, the R_g values are estimated to 30 nm for sphere and 49 nm for rod. Using these equations and the R_g values, we examine to estimate the shape of the PVP−PDP aggregate in the solution. Figure 4 shows the comparison of the experimental SAXS profile with the scattering profiles calculated by assuming spherical or rodlike aggregates for the PVP−PDP(5.0) taking the sol situation. The SAXS profiles calculated for the spherical aggregate with R = 39 nm is not agree with the experimental SAXS profile. On the other hand, when R_c = 12 nm and L = 170 nm, the SAXS profile calculated for the rodlike aggregate is well fitted with the experimental SAXS profile, although the curves are not fitted in high q range due to effect of thermal diffuse scattering on the experimental SAXS profile. The experimental SAXS profile is not adjusted with calculated scattering profiles using the other pairs of R_c and L which satisfy eq 6. For example, SAXS profiles calculated with R_c = 10 and 14 nm are shown in Figure 4. As can be seen in Figure 4, the experimental SAXS profile is fitted only with the scattering profile calculated using R_c = 12 nm and L = 170 nm. The calculated SAXS profiles are not sensitive to the L value because the feature of the scattering profiles is dominated by $J_1(qR_c)$ in eq 5. Hence, among the combinations of R_c and L that satisfy eq 6, only the pair of R_c = 12 nm and L = 170 nm can be fitted to the experimental SAXS profile of the PVP−PDP(5.0).Therefore, in the toluene solution, the PVP−PDP mixture forms the rodlike aggregate with R_c = 12

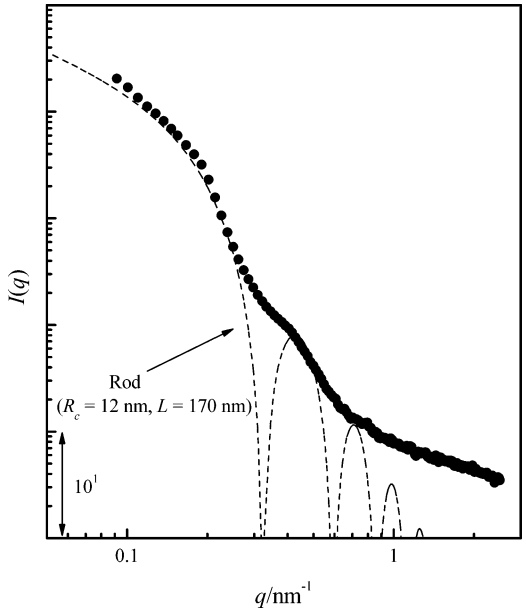

Figure 5. Experimental and calculated SAXS profiles for PVP−PDP(10). Dashed line is calculated by assuming rodlike micelle with $R_c = 12$ nm and $L = 170$ nm.

nm and $L = 170$ nm in the sol situation. The anisotropy of the shape of the PVP−PDP aggregate should be caused due to existence of large amounts of the PDP and toluene, segregation force between the PVP and the others, and strong hydrogen bond between PVP and PDP. The PVP−PDP(10) at the gelation concentration also shows a similar SAXS profile to the PVP−PDP-(5.0). Therefore, it is expected that the experimental SAXS profile of the PVP−PDP(10) is well fitted with the scattering function well fitted with the experimental profile of the PVP−PDP(5.0).

Figure 5 shows the comparison of the experimental SAXS profile of PVP−PDP(10) with the profile calculated by assuming the rodlike aggregates with $R_c = 12$ nm and $L = 170$ nm. As can be seen in Figure 5, the calculated SAXS profile is well fitted with the experimental SAXS profile of the PVP−PDP(10). The positive deviation of the experimental SAXS profile from the calculated profile should reflect interference between the rodlike aggregates. This result indicates that the rodlike form of the PVP−PDP aggregate in the gel situation is identical with that in the sol situation. Therefore, the gelation of the solution is caused because the solutions should cross the percolation threshold where the rotation of each rodlike aggregate is prevented by the other aggregates around 10 wt % of the PVP−PDP aggregates.

Summarizing the results of the SAXS analyses, the aggregation behavior of the toluene solution of the PVP−PDP mixture is schematically represented as Figure 6. The hydrogen-bonded PVP−PDP mixture forms the rodlike micelle with $R_c = 12$ nm and $L = 170$ nm in the toluene solution. Because the R_c value is closely corresponding to R_g of the PVP, the cross-sectional area of the core of the rodlike micelle corresponds to the size of one PVP coil. Therefore, the core of the rodlike micelle should be constructed by about 15 PVP coils. With increasing concentration of PVP−PDP mixture in the solution, interference between the rodlike micelles is caused. Because the interference between the rodlike micelles becomes to prevent the rotation of each micelles with increasing the concentration, the solutions of the PVP−PDP mixture should change the situation from sol to gel with increasing the concentration. However, because the length of the rodlike micelle in the PVP−PDP micelle is relatively short, the relatively high concentration (10 wt %) is need to form the gel.

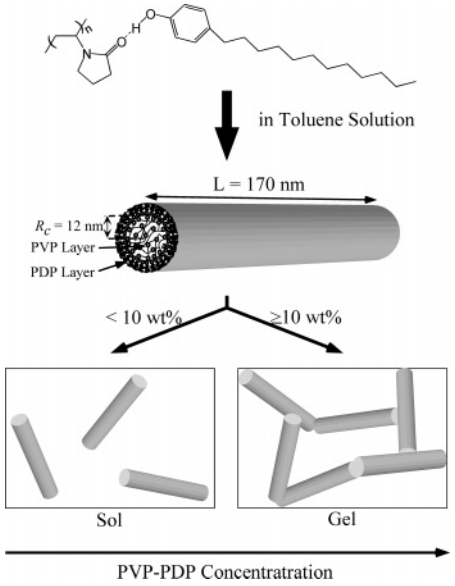

Figure 6. Schematic representation of rodlike micelle formation and gelation in toluene solution of PVP−PDP mixture.

Acknowledgment. SAXS experiments were performed under the approval of the SPring-8 Advisory Committee (approved number 2004A0046-NL2b-np). FTIR measurements were performed at the Instrumentation Center of The University of Kitakyushu. This work is supported by funding from the MEXT via the Kitakyushu Knowledge-based Cluster Project.

References and Notes

(1) MacKnight, W. J.; Ponomarenko, E. A.; Tirrell, D. A. *Acc. Chem. Res.* **1998**, *31*, 781.
(2) Thünemann, A. F. *Prog. Polym. Sci.* **2002**, *27*, 1473.
(3) Ikkala, O.; Ruokolainen, J.; ten Brinke, G.; Torkkeli, M.; Serimaa, R. *Macromolecules* **1995**, *28*, 7088. (b) Vikki, T.; Ruokolainen, J.; Ikkala, O. T.; Passiniemi, P.; Isotalo, H.; Torkkeli, M.; Serimaa, R. *Macromolecules* **1997**, *30*, 4064. (c) Mäki-Ontto, R.; de Moel, K.; Polushkin, E.; van Ekenstein, G. A.; ten Brinke, G.; Ikkala, O. *Adv. Mater.* **2002**, *14*, 357.
(4) Kato, T.; Fréchet, J. M. J. *Macromolecules* **1989**, *22*, 3818. (b) Kato, T.; Nakano, M.; Moteki, T.; Uryu, T.; Ujiie, S. *Macromolecules* **1995**, *28*, 8875.
(5) Ponomarenko, E. A.; Waddon, A. J.; Bakeev, K. N.; Tirrell, D. A.; MacKnight, W. J. *Macromolecules* **1996**, *29*, 4340. (b) Ponomarenko, E. A.; Tirrell, D. A.; MacKnight, W. J. *Macromolecules* **1996**, *29*, 8571. (c) Ponomarenko, E. A.; Tirrell, D. A.; MacKnight, W. J. *Macromolecules* **1998**, *31*, 1584.
(6) Thünemann, A. F.; General, S. *Langmuir* **2000**, *16*, 9634.
(7) Akiba, I.; Akiyama, S. *Macromolecules* **1999**, *32*, 3741. (b) Akiba, I.; Akiyama, S. *Macromolecules* **2000**, *33*, 7967. (c) Akiba, I.; Jeong, Y.; Sakurai, K. *Macromolecules* **2003**, *36*, 8433.
(8) Severin, N.; Rabe, J. P.; Kurth, D. G. *J. Am. Chem. Soc.* **2004**, *126*, 3696.
(9) Lehmann, P.; Kurth, D. G.; Brenzesinski, G.; Symietz, C. *Chem.—Eur. J.* **2001**, *7*, 1646.
(10) Khattari, Z.; Hatta, E.; Kurth, D. G.; Fischer, T. M. *J. Chem. Phys.* **2001**, *115*, 9923.
(11) Fredrickson, G. H. *Macromolecules* **1993**, *26*, 2825.
(12) Akiba, I.; Akiyama, S. *J. Macromol. Sci., Phys.* **2001**, *B40*, 157. (b) Akiba, I.; Seki, T.; Akiyama, S. *e-Polym.* **2002**, 008.
(13) Shibayama, M.; Adachi, M.; Ikkai, F.; Kurokawa, H.; Sakurai, S.; Nomura, S. *Macromolecules* **1993**, *26*, 623.

(14) Feigin, L. A.; Svergun, D. I. *Structure Analysis by Small-Angle X-Ray and Neutron Scattering*; Plenum Press: New York, 1987.
(15) Hirai, M.; Kawai-Hirai, R.; Yabuki, S.; Takizawa, T.; Hirai, T.; Kobayashi, K.; Amemiya, Y.; Oya, M. *J. Phys. Chem.* **1995**, *99*, 6651.
(16) Zhang, J.; Ham, B.; Liu, M.; Liu, D.; Dong, Z.; Liu, J.; Li, D.; Wang, J.; Dong, B.; Zhao, H.; Rong, L. *J. Phys. Chem. B* **2003**, *107*, 3679.
(17) Nakano, M.; Deguchi, M.; Matsumoto, K.; Matsuoka, H.; Yamaoka, H. *Macromolecules* **1999**, *32*, 7437.
(18) Matsumoto, K.; Mazaki, H.; Matsuoka, H. *Macromolecules* **2004**, *37*, 2256.
(19) Schillén, K.; Brown, W.; Johnsen, R. M. *Macromolecules* **1994**, *27*, 4825.

MA0483118